THE RESPONSE OF SUSPENDED PARTICULATE MATERIAL TO UPWELLING AND DOWNWELLING EVENTS IN SOUTHERN LAKE MICHIGAN

CHANG-HEE LEE[1]* AND NATHAN HAWLEY[2]**

[1] *Cooperative Institute for Limnology and Ecosystems Research, University of Michigan, 2200 Bonisteel Blvd., Ann Arbor, Michigan 48109-2099, U.S.A.*

[2] *Great Lakes Environmental Research Laboratory, 2205 Commonwealth Blvd., Ann Arbor, Michigan 48105-1593, U.S.A.*

* *Present address: Daesong Bldg., 1049-1, Sadang-Dong, Dongjak-Gu, Seoul 156-090, Republic of Korea*

** *Author to whom correspondence should be addressed*

ABSTRACT: **Time series measurements of water temperature, beam attenuation, and current velocity were made at three stations located in 28, 58, and 100 m of water off the east coast of Lake Michigan from late August until mid-October 1995. When combined with water intake records and wave measurements our observations show that local resuspension is not responsible for maintaining the benthic nepheloid layer (BNL) during the stratified period. Resuspension of bottom material by surface wind waves occurs in shallow water (13 m), but this material is not transported offshore into the BNL during downwelling events. During upwellings material may be transported onshore from the BNL into shallow water, but additional material is required to produce the concentrations observed at the inner stations. Resuspension by internal waves may be the source of this additional material. Changes in the vertical structure of the benthic nepheloid layer appear to account for most of the changes in suspended particulate material at the two offshore stations. These changes are probably due to a combination of internal wave action and regional changes in current patterns.**

INTRODUCTION

Details of the transport pathways followed by fine-grained material in the Laurentian Great Lakes are poorly understood. Most of this material is introduced into the lakes by either tributaries or shoreline erosion (Rea et al. 1981; Colman and Foster 1994) and then transported to offshore depositional areas (Edgington and Robbins 1990), but exactly how and when this transport occurs is not known. Offshore transport may occur within the benthic nepheloid layer (BNL), which is commonly observed in the deeper parts of the lakes during the stratified period. Chambers and Eadie (1981) suggested that the BNL in Lake Michigan was maintained by a combination of local resuspension and the introduction of nearshore material, and that this material was then transported downslope in the BNL, but the processes responsible for the origin and maintenance of the BNL are also poorly understood. Studies in Lake Ontario (Sandilands and Mudroch 1983; Rosa 1985) and Lake Superior (Baker and Eisenreich 1989; Halfman and Johnson 1989) also cite local resuspension as a means for maintaining the BNL, but Sly (1994) stated that the BNL in Lake Ontario was due mainly to the settling of biogenic material. On the basis of a geochemical study Mudroch and Mudroch (1992) concluded that the particles suspended in the BNL in Lake Ontario were a combination of biogenic and resuspended bottom material. However in none of these investigations was resuspension actually observed. Hawley and Lesht (1995) made time series measurements of current velocity and the concentration of suspended particulate material (SPM) at several stations in Lake Michigan in water depths between 65 and 100 m and found no evidence of local resuspension. Similar findings were reported by Hawley and Murthy (1995) from a station in Lake Ontario located in 65 m of water. Thus, although bottom resuspension has been observed in shallow (< 30 m) in Lake Michigan water (Lesht and Hawley 1987; Lesht 1989), other processes seem to be required to supply material to the BNL in the deeper parts of the lakes. Hawley and Lesht suggested that the BNL is maintained by a combination of vertical mixing of material already in suspension and downslope transport of additional sediment during downwelling events, a process first suggested by Chambers and Eadie (1981).

Boyce et al. (1989) reviewed the seasonal thermal cycle of the lakes and described the various physical processes that occur. Circulation in the lake is driven by the wind, but because of the lake's size rotational forces are important. Storm action is most important during the unstratified period (roughly November–June), when the higher wind speeds and the absence of a thermocline allow the effects of wind action to penetrate deeper into the water column. Shoreline erosion is most active during this period, particularly during the fall before any ice has formed. River input of sediment is greatest during the spring when the snow melts. The lake is stratified from June to November, with a warm epilimnion separated from the colder hypolimnion water (temperature of 4°C) by a thermocline 10–20 m thick. Far fewer storms occur during the stratified period, but upwelling and downwelling events occur frequently. A two-layer circulation system is set up, with the epilimnion responding directly to the wind stress. This causes upwelling and downwelling events to occur as the thermocline tips. On the eastern side of Lake Michigan, winds to the north cause downwelling of surface waters while winds to the south induce upwelling of colder bottom water. These disturbances may then propagate around the lake as internal Kelvin waves (Mortimer 1980; Boyce et al. 1989).

Although downwelling circulation has been cited as an important mechanism for offshore sediment transport, variations in the concentration of suspended particulate material (SPM) and its transport during these events are not well documented. Hawley and Murthy (1995) noted that the concentration of SPM in Lake Ontario varied in response to changes in the vertical structure of the BNL during a strong downwelling event, but found no evidence of downslope transport. However, because their observations were made at a single offshore site, they were not able to determine whether either nearshore local resuspension occurred or whether offshore transport occurred closer to shore. To date, no other observations of SPM concentration during downwelling events have been reported from the Great Lakes. Changes in SPM concentration and its transport during upwelling have received slightly more attention. From an analysis of turbidity and temperature profiles in southeastern Lake Michigan, Bell and Eadie (1983) found that a strong upwelling event reintroduced suspended materials from the offshore BNL into the nearshore area. Time series observations of temperature, currents, and turbidity at a station located in 28 m of water in southeastern Lake Michigan showed that increases in SPM correlated with the passage of upwelling fronts and that the upwelling currents transported SPM upslope (Lesht and Hawley 1987). However, it is not apparent whether the upwelling currents actually cause local resuspension or merely transport materials already in suspension.

This paper reports measurements of temperature, current velocity, and beam attenuation made at three cross-shore mooring sites located in 28 m, 58 m, and 100 m waters in eastern Lake Michigan at the end of the stratified period (late August until mid-October) in 1995. These records are analyzed to identify the causes of major changes in the concentration of SPM and to describe the role of upwelling and downwelling events in the cross-shore transport of this material. In particular we address three previously suggested hypotheses for maintaining the BNL: (1) local resuspension of bottom material by either bottom currents or surface waves maintains the BNL

JOURNAL OF SEDIMENTARY RESEARCH, VOL. 68, NO. 5, SEPTEMBER, 1998, P. 819–831
 1073-130X/98/068-0819/$03.00

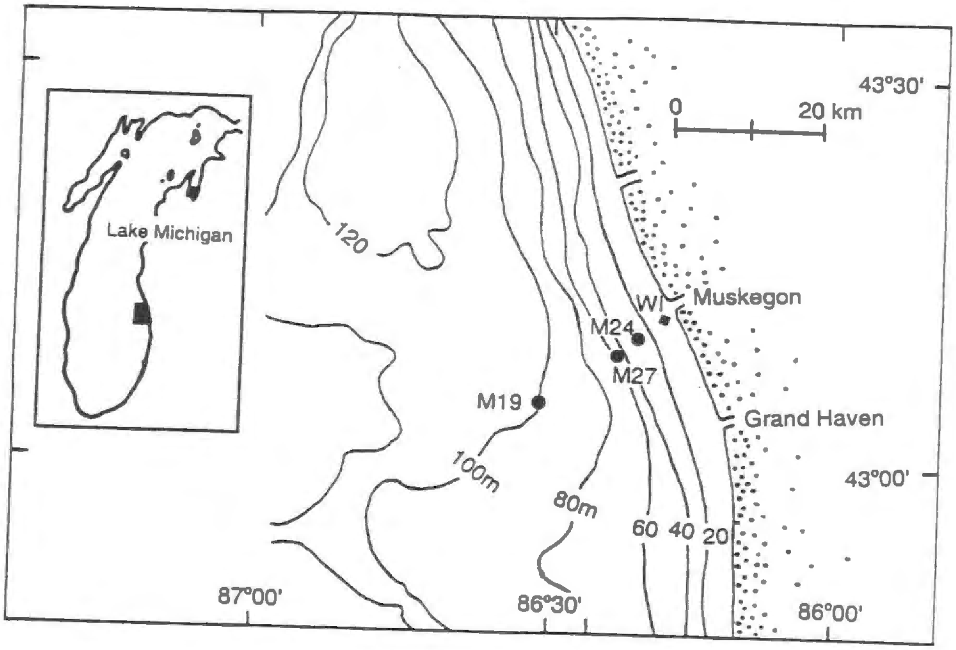

FIG. 1.—Location of the tripod moorings (M24, M27, and M19) and Muskegon municipal water intake (WI). The vertical profiles shown in Figure 2 were made on a transect running from the Muskegon Harbor entrance through the three tripod mooring sites.

during the stratified period, (2) inshore material is resuspended and transported offshore into the BNL during downwelling events, and (3) offshore bottom sediment is resuspended by upwelling currents and transported from the BNL into the epilimnion during upwelling events.

SITE DESCRIPTION AND METHODS

As part of the EPA's Lake Michigan Mass Balance Program, instrumented tripods were deployed at three stations in southern Lake Michigan during 1994 and 1995. The stations were located in water depths of 28 m (M24), 58 m (M27), and 100 m (M19) along a transect that originated in Muskegon, Michigan and ran roughly perpendicular to the shoreline (Fig. 1). Bottom contours in this area (which is near the northern edge of the southern basin of the lake) run roughly parallel to the shoreline, which is oriented northwest to southeast. Depth soundings along the transect show a relatively flat surface to about 30 m depth, then a steeper slope extending to about 80 m before the relatively flat lake bottom is reached. The moorings were deployed and retrieved at slightly different times: M19 was deployed about a week earlier than the other two, and M24 was retrieved about a month after M27 and M19. In this paper we discuss observations made between 29 August and 18 October 1995, although the moorings at both M19 and M27 were retrieved about a week prior to this date. The observations cover the end of the stratified period and the beginning of the annual breakdown of the thermocline. Details of the mooring configurations are summarized in Table 1.

TABLE 1.—*Deployment data*

Station	Water Intake	M24	M27	M19
Deployed	—	28 Aug 1995	29 Aug 1995	22 Aug 1995
Retrieved	—	21 Nov 1995	12 Oct 1995	11 Oct 1995
Latitude	43° 12.30'N	43° 13.75'N	43° 09.50'N	43° 02.93'N
Longitude	86° 20.83'W	86° 25.46'W	86° 25.87'W	86° 38.57'W
Water depth (m)	13	28	58	100
Electromagnetic current measurements				
Height (mab)	—	0.5, 17	0.5, 35	0.5, 35, 65
Sampling rate	—	2 Hz	1 Hz	1 Hz
Sampling per.	—	1 minute/hour	1 minute/hour	1 minute/hour
VACM current measurements				
Height (mab)	—	1, 17	1, 17, 35	1, 17, 35, 65
Sampling rate	—	Continuous	Continuous	Continuous
Sampling per.	—	15 min ave	15 min ave	15 min ave
Temperature measurements				
Height (mab)	3	0.9, 7, 17	0.9, 7, 17, 35	0.9, 7, 17, 35, 65
Sampling rate	Hourly	1 Hz	1 Hz	1 Hz
Sampling per.	Single meas.	1 minute/hour	1 minute/hour	1 minute/hour
Transparency measurements				
Height (mab)	3	0.9, 7, 17	0.9, 7, 17, 35	0.9, 7, 17, 35, 65
Sampling rate	Bi-hourly	1 Hz	1 Hz	1 Hz
Sampling per.	Single meas.	1 minute/hour	1 minute/hour	1 minute/hour
Size analysis				
Percent sand	100	94	55	40
Percent silt	0	5	42	44
Percent clay	0	1	3	16
Mean dia. (cm)	0.026	0.024	0.016	0.014

Marsh–McBirney 585 and Interocean S4 electromagnetic current meters were used to measure current velocities at the three stations. Calibrations made in a towing tank prior to deployment show that the current meters had a resolution of 0.5 cm s^{-1} and an accuracy of 1 cm s^{-1}. EG&G vector-averaging current meters (VACM) were also deployed at the same elevations as the electromagnetic current meters, and an additional VACM was deployed 17 m above the bottom (mab) at stations M27 and M19. The VACMs have a lower threshold of 2 cm s^{-1} and an accuracy of 1 cm s^{-1}. Comparison of the current records shows that the electromagnetic current meters gave essentially the same results as the VACMs except when the current speed was below the VACM threshold. In this paper we have used the results from the electromagnetic current meters except for the 17 mab observations at M27 and M19. Currents were rotated 40° to provide the alongshore and cross-shore components.

Temperature measurements were made using Yellow Springs thermistors accurate to 0.2°C. Water transparency measurements were made using Sea Tech transmissometers (25 cm pathlength) and Sea Tech light-scattering sensors (LSS). The transmissometer and light-scattering sensor readings were recorded to the nearest 0.001 volt over a nominal 5 volt scale. Although the readings of both the transmissometers and the LSS respond to changes in the suspended sediment concentration, we found that each LSS responded differently to changes in sediment concentration when compared to the beam attenuation coefficient (BAC, which is independent of the instrument used) computed from the transmissometer readings. Bottom material from M27 was used to perform a five-point calibration between the voltage reading for each LSS and the BAC measured by a transmissometer. These data were then used to construct a separate correction equation for each of the LSS. The correction equations varied significantly from sensor to sensor, but the r^2 values were all greater than 0.99. In this paper we use BAC as a surrogate for suspended particulate material (SPM). All instruments (except for the VACMs, which recorded a continuous 15-minute average) were sampled at 1 Hz for 1 minute every 1 hour; the averaged values and their standard deviations were then recorded.

We also used the temperature and water turbidity records made at the Muskegon municipal water intake (WI in Fig. 1). The water intake is located approximately 1.5 km offshore in 13 m of water and is 3 mab. Temperature was measured hourly, but because turbidity was measured every other hour an averaged value between each two measurements was used to obtain an hourly record. The turbidity readings were reported in nephelometric turbidity units (NTU). These were converted to BAC by determining the BAC at 5 NTU levels and constructing a correction equation. These measurements were made using the same standard turbidity solution used to calibrate the water intake's turbidity meter. Because a time lag of up to 6 hours could exist between the time the water entered the intake and the time that the measurements were made at the station on shore, the intake records were shifted 6 hours prior to plotting. However since the time lag is not constant, the intake data are not always simultaneous with the other measurements. Water intake data were not available for 2 September or 17 September.

Vertical profiles of water temperature and BAC were made weekly on a cross-shelf transect using a Seabird CTD unit equipped with a 25 cm Sea Tech transmissometer. The transect ran from Muskegon Harbor through the mooring sites and included stations in 12 (the Muskegon breakwater), 28 (M24), 45, 58(M27), 80, and 100 m (M19) of water. Although the water depth at the Muskegon breakwater is about the same as that at the water intake, the two sites are several kilometers apart (Fig 1). Wave observations were made using a Datawell waverider buoy located at M24. Measurements were made at 2 Hz for 10 minutes per hour and the average wave period and significant wave height computed. Hourly wind data were obtained from a weather station located at the entrance to Muskegon Harbor.

Bottom sediment samples were collected with a Ponar bottom grab sampler at the water intake station and at the mooring sites. Examination of these samples showed that the bottom material was cohesive at M27 and M19 and noncohesive at M24 and the water intake. The material from the top centimeter was wet sieved to separate the sand fraction (diameter > 0.064 cm) prior to determining the fine-sediment size distribution with a Spectrex model ILI-1000 laser particle counter. The sizes of the coarser material were analyzed with a settling tube. The analyses show that the bulk (over 70%) of the coarser material at all of the stations was medium and fine sand (diameters between 0.5 and 0.125 mm). Results from the size analyses are included in Table 1. Observations made with a remotely operated vehicle show that the bottom is flat (no bedforms) at stations M24, M27, and M19, and rippled at the water intake station.

RESULTS

Temperature profiles made during the deployment (Fig. 2; data from 5, 11, and 18 September, and 5 October are not shown) show that the epilimnion water cooled during the deployment from about 25° to 15°C, and that although the lake as a whole remained stratified throughout the deployment, the water at stations 12 and M24 became isothermal after about 25 September as the thermocline deepened (except for two intervals discussed below). The depth of the thermocline (taken to be the 10° isotherm) also changed several times because of upwelling and downwelling events. This caused the instruments at both M24 and M27 to alternate between being located in the hypolimnion and in the epilimnion. For example, at the beginning of the deployment the 35 mab instruments at M27 were located

TABLE 2.—*Thickness of the BNL (m), total suspended material (g) in a vertical m^2 column extending through the BNL, and the average concentration (mg l^{-1}) of suspended material in the BNL.*

Date		12	M24	45	M27	80	M19
29 Aug	Thickness	12*	13	12	12	27	44
	Total	25.47	27.08	32.03	46.19	85.33	58.79
	Average	2.13	2.08	2.67	3.85	3.16	1.34
5 Sept	Thickness	12*	11	30	37	33	36
	Total	32.09	20.02	92.76	88.78	62.52	100.45
	Average	2.67	1.82	3.09	2.40	1.89	2.79
12 Sept	Thickness	12*	19	32	28	40	37
	Total	27.51	40.43	77.53	72.05	75.16	76.64
	Average	2.29	2.13	2.42	2.57	1.88	2.07
18 Sept	Thickness	—	28*	—	36	—	40
	Total	—	49.47	—	125.47	—	87.89
	Average	—	1.77	—	3.48	—	2.20
25 Sept	Thickness	12*	14	21	28	51	72
	Total	28.78	23.80	63.67	67.26	254.69	112.54
	Average	2.40	1.70	3.03	2.40	4.99	1.56
4 Oct	Thickness	12*	28*	11	33	14	54
	Total	17.86	38.08	26.07	64.33	41.61	53.46
	Average	1.49	1.36	2.37	1.95	2.97	1.00
11 Oct	Thickness	12*	28*	19	21	38	64
	Total	18.05	28.29	34.31	49.51	80.97	67.47
	Average	1.50	1.01	1.81	2.36	2.13	1.05

Data for station 12 were collected in the Grand River plume and are included for comparison purposes only.

* Indicates data is for the entire water column

in the hypolimnion, but on 25 September they were located in the epilimnion. This complicates the analysis somewhat since the currents in the two water masses are different. At M19 all but the 65 mab instruments were always located in the hypolimnion.

The BAC profiles show that a BNL existed in the hypoliminion at all of the stations whenever the water was at least slightly stratified, but that it was never present in the epilimnion. Both the thickness of the BNL (the top of the BNL is defined as the height where the BAC reaches a minimum value) and the amount of suspended material contained within it varied greatly with both time and location. At the beginning of the deployment the BNL was relatively thin and well-defined at the outer stations, but as the thermocline deepened the BNL thickened and became increasingly diffuse so that by the end of the deployment it occupied the entire hypolimnion. To estimate the amount of material suspended in the BNL, BAC values were first converted to suspended material concentration on the basis of Hawley and Zyrem's (1990) equation and then integrated from the bottom to the top of the BNL These values (Table 2) show that there is considerable variation with time in the total amount of suspended material—particularly at the deeper stations—and that the average concentration of suspended material was highest at the stations located on the lake slope (stations 45, M27 and 80). Hawley and Zyrem estimated the uncertainty of their equation to be 10–20%, so the errors in these calculations are of that magnitude.

Winds were fairly strong during almost the entire period and changed direction numerous times (Fig. 3A). Maximum wind speeds of over 15 m s^{-1} occurred on 16 October and speeds of over 12 m s^{-1} occurred on several other occasions. The wave heights and wave periods measured at M24 (Fig. 3B) are directly correlated with wind speed and wind direction. Strong winds from the north and northwest generated the largest waves because the fetch is longest in these directions. This means that large waves are likely to be associated with upwelling events in this part of the lake. The significant wave height reached a maximum on 15 October, when it exceeded 3 m, and there were several other occasions when it exceeded 2 m. Wave periods between 4 and 6 s occurred several times during the deployment. Linear wave theory predicts that the effects of surface waves with a period of 6 s or greater should reach to the bottom in 28 m of water, which is the depth at M24.

In addition to surface waves, the wind activity generated both near-inertial internal waves and a series of upwelling and downwelling events. Near-inertial internal waves are responsible for the short-period oscillations seen in the temperature records. These waves were common prior to 25 September, but they also occurred in the 7 mab temperature record for 6–10 October and at 17 mab on 16 October. Since these waves can exist only in a stratified fluid, their presence indicates that the water column at M24 became re-stratified during these periods. The upwellings and downwellings are most clearly seen in the temperature records at the water intake and M24 (Fig. 3C–F). These temperature changes coincide with the wind events (although there is a lag time), so they are probably locally generated and are not due to propagation of internal Kelvin waves around the lake. Computer simulations of the thermal structure of the lake also show no Kelvin waves during the deployment (Schwab and Beletsky 1997). Table 3 lists the approximate start and end (based mainly on the 7 mab temperature observations at M24) of the upwellings and downwellings identified in Figure 3. The temperature records at the water intake and M24 show that the point at which the thermocline intersected the bottom moved back and forth past the stations several times during the deployment. Temperatures are highest at the water intake and 17 mab at M24, but even these records show several instances when colder hypolimnion water was present. Temperatures at the two bottom elevations at M24 show that hypolimnion water was present most of the time until 24 September, after which warmer water was present throughout the water column. This is when the water column first became well mixed at M24. The absence of near-inertial oscillations after this date (except during the upwellings on 6–10 and 16 October) supports this inference. CTD profiles made on 5 October are almost identical to those on 11 October (Fig. 2C), so it is likely that the water column was unstratified between both 25 September–6 October and 10–15 October. Lake surface temperature observations made by satellite on 16 and 17 October show that the surface water temperature was about 16°C on both days, so the water column at M24 was stratified after the passage of the cold front on 16 October and unstratified after the warm front passed on 17 October.

The near-inertial internal waves (period of about 17.6 hr) also cause the rotary motions seen in the current velocities at M24 and M27 (Fig. 4). The 17 mab currents at M24 are aligned with the wind direction most of the time, as would be expected since most of these observations were made in the epilimnion, where the currents are driven by the wind. On the few occasions when the sensor was in the hypolimnion (where a compensating return flow develops), the currents are opposite to the wind direction. The bottom currents are more variable but are mainly in the direction opposite to that of the wind except when the water column was unstratified or when the sensor was in the epilimnion. Currents at both elevations are predominantly alongshore, but at 17 mab northward currents generally have an onshore component while southward currents usually have an offshore component. At 0.5 mab the currents are almost exclusively northward, but when the sensors were in the epilimnion the currents are similar to those 17 mab. When the measurements were made in the hypolimnion, the currents are mainly to the north and slightly offshore.

The water intake record (Fig. 3F) shows that most of the BAC peaks occurred simultaneously with an increase in wave activity (represented by the bottom wave shear stress) and then decreased to background levels when the waves ceased. The stresses shown at the water intake were calculated using linear wave theory and the wave parameters measured at M24. We have used these values rather than the stress due to combined waves and currents because we have no current measurements from this location. Two major wave-induced resuspension events occurred during the observation period (on 22 September and 14–15 October) as well as several smaller ones. During most of the BAC peaks the wave stress far exceeded 1.5 dynes cm^{-2}, which is about the value needed to resuspend fine sand (Miller et al. 1977). The largest BAC peak (on 16 October) occurred after the peak in wave shear stress and is associated with the passage of a cold front. Except for this peak, the BAC data can be explained by local resuspension due to surface wave action.

The BAC observations at the three elevations at M24 (Fig. 3C–E) are similar to each other even when the observations were made in different water masses. The two largest BAC events at the intake station (those on 22 September and 14–16 October) are also clearly evident at this station, although the peak levels are considerably less than at the water intake. The bottom shear stresses due to waves and currents (Fig. 3E) were calculated by the model of Kim et al. (1997) using the wave observations and the 0.5 mab current meter data as input parameters. This model is a modified version of the Grant and Madsen (1979) model. We used the mean grain size (0.024 cm) as the bottom roughness parameter required by the model. The bottom stresses reach a maximum value of about 1.73 dynes cm^{-2} on 14 October, but otherwise exceed 1 dyne cm^{-2} on only a few occasions, none of which coincide with a peak in BAC. The bottom stress on 22 September was far too low to resuspend bottom material, but the stress on 14 October was probably sufficient. However, the BAC peak actually occurred several hours after the peak stress and coincided with the passage of a cold front several hours later on 15 October. The bottom current velocity record at M24 (Fig. 4F) shows that the direction changed from alongshore to onshore at exactly the same time as the decrease in temperature and the increase in BAC. This cold front is the same one that caused the BAC peak at the intake station on 16 October.

On 22 September the BAC at all levels increased as the water temperature decreased, but since the bottom stress remained low, it is unlikely that local resuspension occurred. These changes occurred near the bottom first and then higher in the water column as the cold front passed the station. Currents in the colder hypolimnion water were slightly onshore, as would be expected during an upwelling event, so it is unlikely that material

→

FIG. 2.—Vertical profiles of water temperature in °C (dashed line) and beam attenuation coefficient (solid line) observed at stations in 12, 28 (M24), 45, 58 (M27), 80, and 100 (M19) m of water. Elevations of the time series observations are shown by the horizontal dotted lines. **A)** Profiles made on 29 August 1995. **B)** Profiles made on 25 September 1995. **C)** Profiles made on 11 October 1995.

FIG. 3.—Time series data from the water intake and M24. In Figures C, D, E, and F the black line is the beam attenuation coefficient, the blue line is the temperature, and the red line is either the current speed or the bottom shear stress. Current speeds are in cm s^{-1}, temperatures in °C, shear stress in dynes cm^{-2}, and BAC in m^{-1}. The dotted vertical lines separate the upwelling and downwelling events listed in Table 3. **A)** Wind at the weather station at the entrance of Muskegon Harbor. The convention is that wind blows in the direction of the line, so the wind on 29–30 September blew from the south to the north. **B)** Wave height in meters (black), and wave period in seconds (blue) at M24. **C)** Beam attenuation, temperature, and current speed measured at 17 mab at M24. No attenuation measurements are available after 9 October. **D)** Beam attenuation and temperature measured at 7 mab at M24. Speed is that at 0.5 mab. **E)** Beam attenuation and temperature at 0.9 mab, and bottom stress due to combined wave and current action at M24. **F)** Beam attenuation, water temperature, and bottom stress due to wave action at the water intake. Beam attenuation and temperature were measured at 3 mab. No data are available for 2 or 17 September.

FIG. 4.—Current velocities at M24 and M27. The current velocities have been rotated 40° clockwise so that alongshore is up and down and offshore is to the left. The convention is that the wind and currents go the direction of the line, so the wind on 29–30 September blew from the south to the north. The dotted vertical lines separate the upwelling and downwelling events listed in Table 3. **A)** Wind at the weather station at the entrance of Muskegon Harbor. **B)** Current velocity 35 mab at M27. **C)** Current velocity 17 mab at M27. **D)** Current velocity 0.5 mab at M27. **E)** Current velocity 17 mab at M24. **F)** Current velocity 0.5 mab at M24.

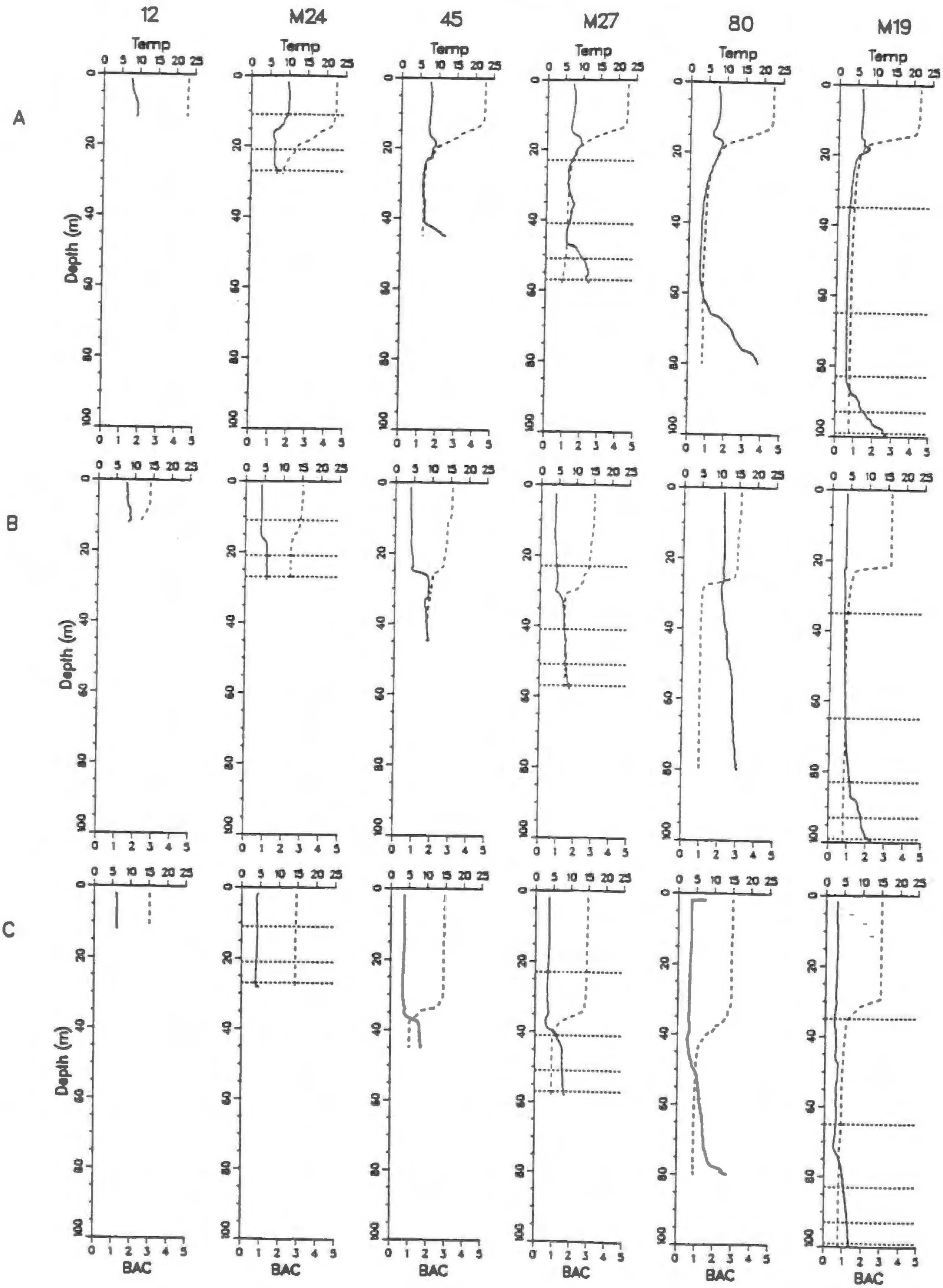
12
M24
45
M27
80
M19
A
B
C
Temp
Depth (m)
BAC
0 5 10 15 20 25
0 1 2 3 4 5
0 20 40 60 80 100

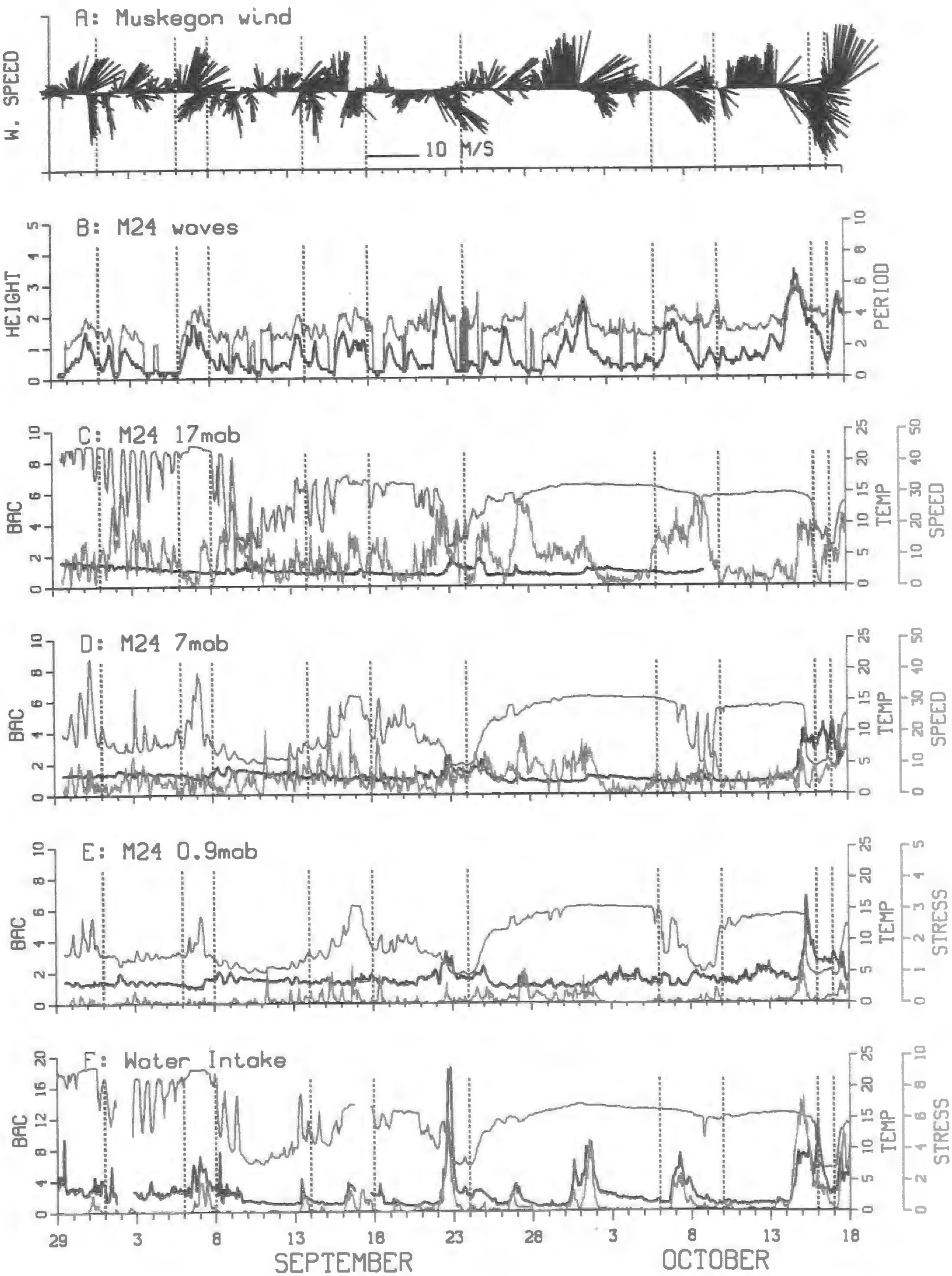
A: Muskegon wind
W. SPEED
10 M/S
B: M24 waves
HEIGHT
PERIOD
C: M24 17mab
BAC
TEMP
SPEED
D: M24 7mab
BAC
TEMP
SPEED
E: M24 0.9mab
BAC
TEMP
STRESS
F: Water Intake
BAC
TEMP
STRESS
29
3
8
13
18
23
28
3
8
13
18
SEPTEMBER
OCTOBER

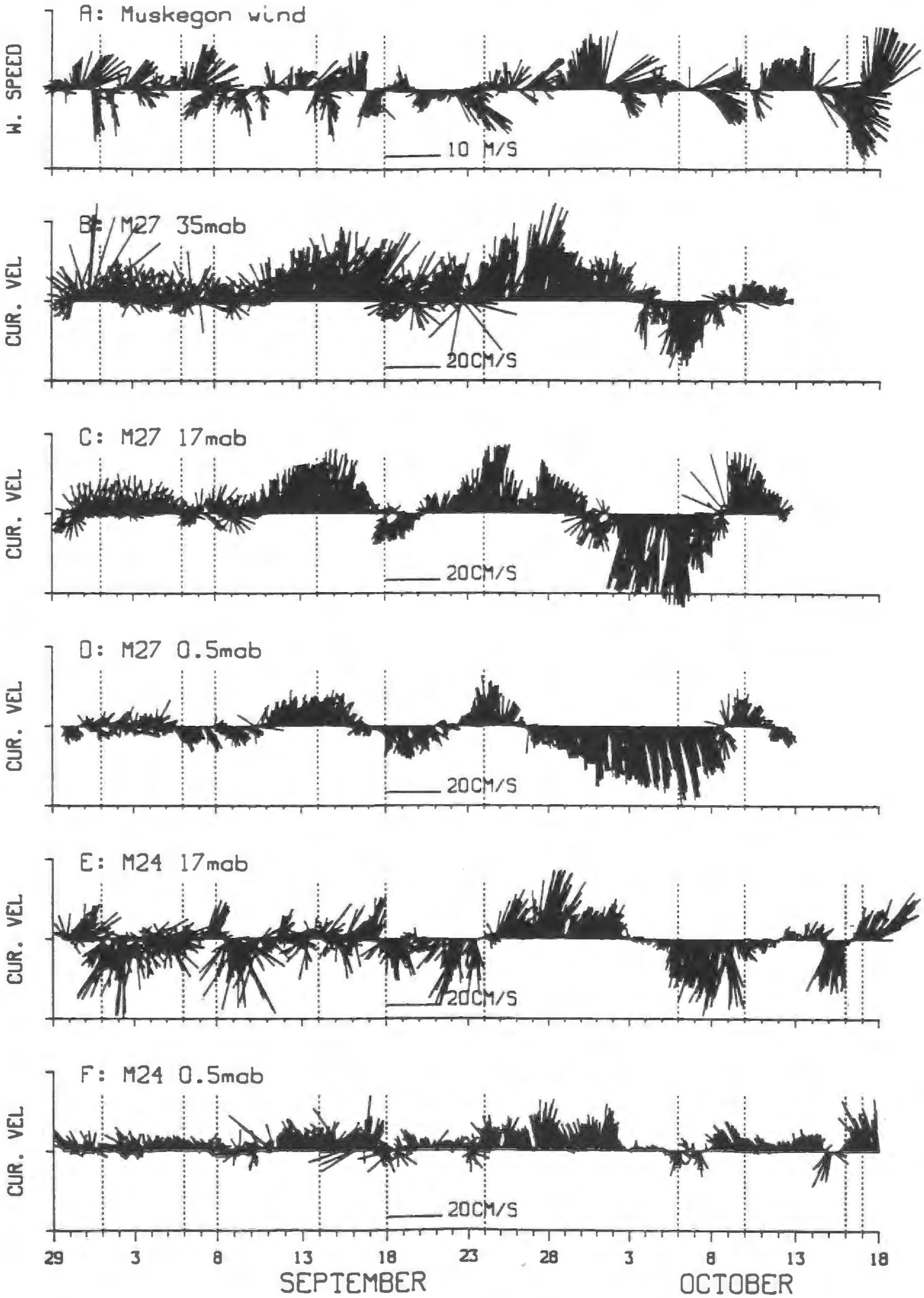
A: Muskegon wind
W. SPEED
10 M/S
B: M27 35mab
CUR. VEL
20CM/S
C: M27 17mab
CUR. VEL
20CM/S
D: M27 0.5mab
CUR. VEL
20CM/S
E: M24 17mab
CUR. VEL
20CM/S
F: M24 0.5mab
CUR. VEL
20CM/S
29 3 8 13 18 23 28 3 8 13 18
SEPTEMBER
OCTOBER

TABLE 3.—*Upwelling and downwelling events at M24*

Dates	Water Column Stratified or Unstratified	Upwelling or Downwelling	Predominant Wind Direction	17 Mab Sensor Located in Epilimnion or Hypolimnion	Current Direction 17 Mab	0.5 Mab Sensor Located in Epilimnion or Hypolimnion	Current Direction 0.5 Mab
29 August–1 September	Stratified	Downwelling	to the north	epilimnion	north	hypolimnion	north
1 September–6 September	Stratified	Upwelling	to the south then north	epilimnion	south	hypolimnion	north
6 September–8 September	Unstratified	Downwelling	to the north	epilimnion	north	epilimnion	north
8 September–14 September	Stratified	Upwelling	to the south, then north	both	south, then north	hypolimnion	north
14 September–18 September	Unstratified	Downwelling	to the north, then south	epilimnion	north	epilimnion	north
18 September–24 September	Stratified	Upwelling	to the north, then south	epilimnion, hypolimnion	south	hypolimnion	north
24 September–6 October	Unstratified	Downwelling	to the north	epilimnion	north, then south	epilimnion	north
6 October–10 October	Stratified	Upwelling	to the south, then north	epilimnion	south	hypolimnion	south, then north
10 October–16 October	Unstratified	Downwelling	to the north	epilimnion	north, then south	epilimnion	north, then south
16 October–17 October	Stratified	Upwelling	to the south	hypolimnion	north	hypolimnion	north
17 October–18 October	Unstratified	Downwelling	to the north	epilimnion	north	epilimnion	north

resuspended at the water intake was transported to the site. On 14 October the initial increase in BAC occurred simultaneously with the peak in bottom stress, so some local resuspension may have occurred, but the highest BAC levels coincided with the passage of the cold front several hours later. Thus although local resuspension may have occurred, the bulk of the increased BAC was associated with onshore transport during an upwelling event.

The records of both temperature and current speed at M27 show the presence of near-inertial waves throughout the deployment (Fig. 5). In contrast to M24, the temperature profiles (Fig. 2) indicate that the water at this station remained stratified throughout the observation period. Large changes in temperature are not as evident near the bottom, so the upwelling events seen at M24 are most apparent in the 35 mab record, which is very similar to the 17 mab record at M24. The temperature records at 7 and 17 mab both show the downwelling event observed at M24 on 24 September and the upwelling that started on 6 October, although the starting times are not the same.

BAC observations at this station are generally somewhat higher than those at M24 and are similar to each other, but since there is no correlation with the bottom current stress, local resuspension did not occur—even though the bottom stress reached 2 dynes cm^{-2} on 6 October (this stress was calculated from the near-bottom current speed by assuming a logarithmic velocity profile and a bottom roughness of 0.016 cm). Nor is there a correlation between BAC and temperature, as there is at M24. BAC levels show a gradual increase and decrease between 13 and 23 September at the three lower elevations, but there is no correlation with the passage of thermal fronts.

Current velocities at the three elevations (Fig. 4) are similar to each other and slightly resemble the 17 mab currents at M17. The rotary motion due to near-inertial internal waves is particularly evident at the two upper elevations but can also be seen in the 0.5 mab record. Otherwise the currents were almost completely alongshore at all three heights, but at the upper two elevations there was a slight onshore component when the currents flowed to the north and a slight offshore component when the current flowed to the south. In the bottom record there was a slight onshore component regardless of the alongshore direction. Changes in direction generally occurred at about the same time at all three elevations except for the change from north to south that occurred after 26 September. This change occurred at the bottom first but not until about 5–7 days later at the upper elevations. Unlike at M24 the changes in current direction do not correlate well with changes in temperature.

Because all of the observations at M19 (except at 65 mab) were made well below the thermocline, there is little indication in the temperature records of either near-inertial waves or thermal fronts (Fig. 6). The only exception is a downwelling event beginning on 6 October. The oscillations in the current speeds show however that near-inertial waves were present throughout the deployment. The bottom current speeds are low (maximum bottom stress is much less than 1 dyne cm^{-2}, for a bottom roughness of 0.014 cm) and show little correlation with BAC, so bottom resuspension is unlikely to have occurred. BAC at M19 varied relatively little during the deployment, but the observations at the bottom three elevations are very similar to one another and to those at M27. As at M27, the BAC shows no correlation with the current speed. Current velocities at M19 (Fig. 7) show pronounced near-inertial motions, and have a much larger onshore–offshore component than those at M24 and M27. The general pattern of the currents is similar at all four elevations, and the bottom currents at M19 are similar to the bottom currents at M27, although the speeds are much lower. Currents at 65 mab show a change in current direction from south to north on 7 October, the same time as the only large increase in temperature. The current direction then changed from north to south on 11 October, when the temperature decreased.

DISCUSSION

The simultaneous increases of BAC and wave stress observed at the water intake clearly show frequent wave-induced local resuspension: Lesht (1989) reported similar activity at a station located at about the same depth in the southern part of the lake. The offshore extent of wave-generated resuspension depends on wave intensity, water depth, and the resistance to erosion of the bottom sediments. Our observations indicate that wave-induced resuspension is confined to relatively shallow waters. Estimated maximum bottom stresses at M24 are about 0.5 and 1.73 dynes cm^{-2} on 22 September and 14 October, respectively. Because the critical bed shear stress required to erode fine sand is about 1.3–1.5 dynes cm^{-2} (Miller et al. 1977), only the waves on 14–15 October (when the water was unstratified) were sufficient for local resuspension. A survey of the Lake Michigan wave records (Transport Canada 1991) shows that waves larger than those on 14–15 October (about 3.4 m in significant height and 6.0 s average period) constitute only about 5% of the total wave record each year, with the majority of the large waves occurring during the winter. If our observations are representative, then local resuspension due to surface wind waves rarely occurs in water deeper than 28 m during the stratified period.

Observations at stations M27 and M19 (58 m and 100 m) show no evidence of current-induced local resuspension. The maximum calculated bottom stress at M27 is about 2 dynes cm^{-2}, which is considerably greater than that needed to erode fine sand, but the actual bottom roughness length may be less than that used to compute the shear stress (0.016 cm, the mean grain size). Since the sediment is poorly sorted the smaller particles may partially shield the larger ones from the flow, thus reducing the roughness seen by the fluid. However even if a roughness of 0.005 cm is used the maximum stress is 1.48 dynes cm^{-2}. While lower than the original estimate, this stress is still high enough to resuspend fine sand, but mixtures of sand and silt can be considerably more resistant to erosion than either pure sand or pure silt (Mitchener et al. 1996; Panagiotopoulos et al. 1997). The maximum bottom stress at M19 is much less than 0.5 dynes cm^{-2}, so no resuspension would be expected. Hawley and Lesht (1995) also found no evidence of local resuspension in several months of time series observations in the hypolimnion (65–100 m of water) of Lake Michigan. Although local resuspension has been suggested as an important mechanism for maintaining the offshore BNL (Eadie et al. 1984; Baker and Eisenreich 1989), these results indicate that current-induced local resuspension rarely occurs in the offshore hypolimnion water during the stratified period. Thus our hypothesis that local resuspension by either surface waves or bottom currents is responsible for maintaining the BNL during the stratified period is probably not true.

The horizontal sediment flux can be calculated from the time series observations by converting the BAC to total suspended material (using the equation given by Hawley and Zyrem 1990) and then multiplying by the cross-shore component of the current velocity. Since the variations in BAC at M24, M27, and M19 (we have no current measurements at the water intake) are much less than the velocity changes, the calculated fluxes closely resemble the currents shown in Figures 4 and 7. The effect of the rotary motions due to internal waves causes both onshore and offshore transport during both upwelling and downwelling events at all three stations, but the cumulative flux is offshore near the bottom at M24 and onshore at M27. Although there is some offshore transport during downwelling events, the relatively low BAC levels at M24 indicate that any local resuspension (as seen at the water intake) and subsequent offshore transport are mostly confined to areas farther inshore. The increased BAC on 25 September indicates that material resuspended in shallow water can be transported farther offshore during some downwelling events; a similar episode during a downwelling is also seen in Lesht and Hawley's (1987) observations. It is unlikely, however, that the material is transported directly into the offshore BNL as proposed by Chambers and Eadie (1981) and Hawley and Lesht (1995). Our temperature records show that the bottom water at M27 was always in the hypolimnion—even when the 7 mab temperature increased on 28 September. Although there is an increase in the bottom BAC at this time, the bottom currents are onshore, so it is unlikely that direct transport of material across the thermocline into the hypolimnion occurred. Since previous studies in Lake Ontario show that downwelling events are restricted to a nearshore zone of about 4–8 km from shore (Csanady and Scott 1974; Blanton 1975), and since no evidence of downslope transport was found at a 60 m station during a strong downwelling (Hawley and Murthy 1995), it seems unlikely that direct transport of inshore material into the BNL occurs even during strong downwelling events, unless it occurs nearer shore. Churchill et al. (1988) observed offshore transport of material due to frontal movements, but their observations seem to better resemble the processes that occur between the water intake and M24, rather than between M24 and M27. On longer time scales settling of the transported material from the epilimnion may eventually contribute to the offshore BNL, but direct offshore transport of material to the hypolimnion during downwellings does not seem to occur. Thus our second hypothesis is also incorrect, at least at our stations. It is possible that resuspension and offshore transport could occur on the west side of the lake, where the largest waves would be associated with downwelling—rather than upwelling—events.

The largest increases in BAC at M24 are mostly due to reintroduction of relatively turbid offshore hypolimnion water during upwelling events, as described by Bell and Eadie (1983). Our observations show that temperature drops at M24 are associated with onshore bottom currents, and that near-bottom BAC values during the deployment are generally higher at the offshore stations than at M24. However, increases in BAC at M24 during the passage of cold water fronts cannot be due solely to reintroduction of the offshore hypolimnion water because the increased BAC is often higher than that observed farther offshore, and because the increased BAC drops again as soon as the front has passed. Because the current speeds are low (Figs. 3 and 4), it is unlikely that upwelling currents by themselves initiate local resuspension, but clearly some additional material is required to produce the BACs observed at M24 on 16 October.

If we use the BAC at 7 mab on October 16 to compute the total amount of material in suspension at M24 the result is 185 g. This far exceeds the amount of material measured in any of the profiles at either M27 or at the 45 m station. If we compute the average value of the BAC required to equal this load in a BNL 35 m thick, then the BAC required is about 3.3 m^{-1}, which is about the maximum value recorded during the deployment at M27. However this value is never reached at 17 mab or at 35 mab, so considerably more material would need to be in suspension than was ever observed. The vertical profile made on 11 October shows that the total amount of material suspended in the BNL at M27 was only about 50 g—less than 30% of the amount required. This means that whatever process is responsible for the increased BAC at M24 must cause considerable local resuspension. Breaking internal waves may be the cause. A recent study by Bogucki et al. (1997) documented sediment resuspension by breaking internal solitary waves during an upwelling on the California shelf. If similar processes occur in the Great Lakes, they could explain the high BAC levels observed. Unfortunately, our data do not allow us to determine whether breaking internal waves were present, but it seems clear that upwelling currents by themselves do not resuspend bottom material, so our third hypothesis is also incorrect.

Variations of near-bottom BAC at the offshore stations mainly reflect changes in the vertical structure of the BNL, because no evidence of either local resuspension or of downslope sediment transport was observed. Vertical mixing of the BNL (as described by Hawley and Lesht 1995) is at least partly responsible for the changes in BAC observed at M27 and M19. No relationship between near-bottom BAC and either current direction or temperature is readily apparent at either M27 or M19, but there are distinct similarities in both the bottom current velocities and the BAC at the two stations. These changes are probably not due to a site-specific local response, but more likely are due to regional changes in the circulation patterns. The relatively uniform changes in the BNL with time (as seen in Fig. 2) also suggests regional rather local processes. On shorter time scales internal waves are probably also important in changing the structure of the BNL, but without additional vertical profiles it is hard to determine their effects.

Our observations, when coupled with those of previous studies (Lesht and Hawley 1987; Hawley and Lesht 1995; Hawley and Murthy 1995), show that resuspension episodes are usually confined to quite shallow water (approximately 13 m) during the stratified period. The combination of a strong thermocline, which inhibits the transfer of wind energy to the bot-

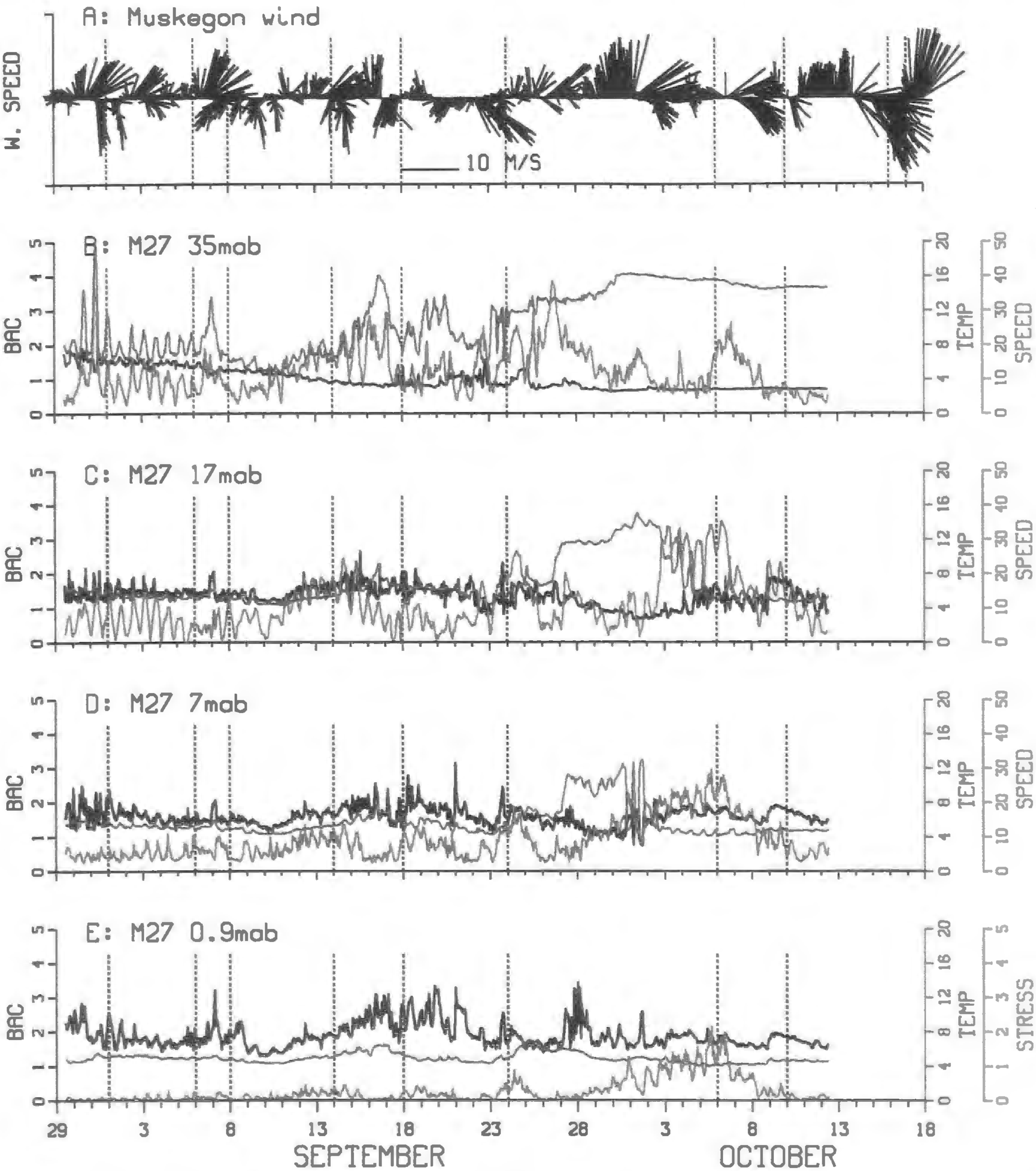

FIG. 5.—Time series data from station M27. Beam attenuation is shown by the black line, temperature by the blue line, and current speed or shear stress by the red line. Current speeds are in cm s^{-1}, stress in dynes cm^{-2}, temperatures in °C, and BAC in m^{-1}. The dotted vertical lines separate the upwelling and downwelling events listed in Table 3. **A)** Wind at the weather station at the entrance of Muskegon Harbor. The convention is that wind blows in the direction of the line, so the wind on 29–30 September blew from the south to the north. **B)** Beam attenuation, temperature, and current speed measured at 35 mab. **C)** Beam attenuation, temperature, and current speed measured at 17 mab. **D)** Beam attenuation and temperature measured at 7 mab, current speed measured 0.5 mab. **E)** Beam attenuation and temperature measured at 0.9 mab, and bottom shear stress due to current action.

→

FIG. 6.—Time series data from station M19. Beam attenuation is shown by the black line, temperature by the blue line, and current speed or bottom stress by the red line. Current speeds are in cm s^{-1}, stress in dynes cm^{-2}, temperatures in °C, and BAC in m^{-1}. The dotted vertical lines separate the upwelling and downwelling events listed in Table 3. **A)** Wind at the weather station at the entrance of Muskegon Harbor. The convention is that wind blows in the direction of the line: so the wind on 29–30 September blew from the south to the north. **B)** Beam attenuation, temperature, and current speed measured at 65 mab. **C)** Beam attenuation, temperature, and current

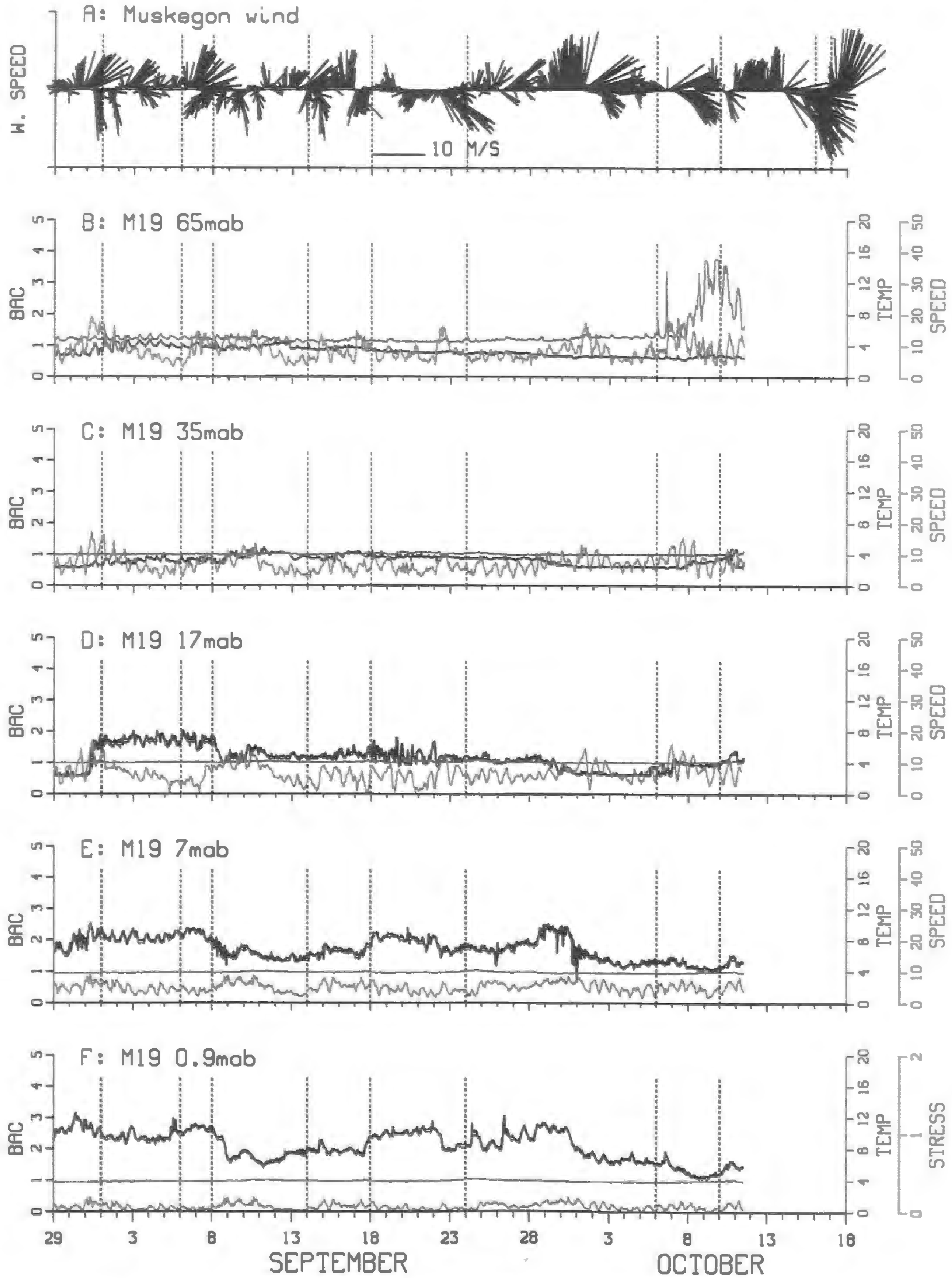

speed measured at 35 mab. **D)** Beam attenuation, temperature, and current speed measured at 17 mab. **E)** Beam attenuation and temperature measured at 7 mab, current speed measured at 0.5 mab. **F)** Beam attenuation and temperature measured at 0.9 mab, and bottom shear stress due to current action.

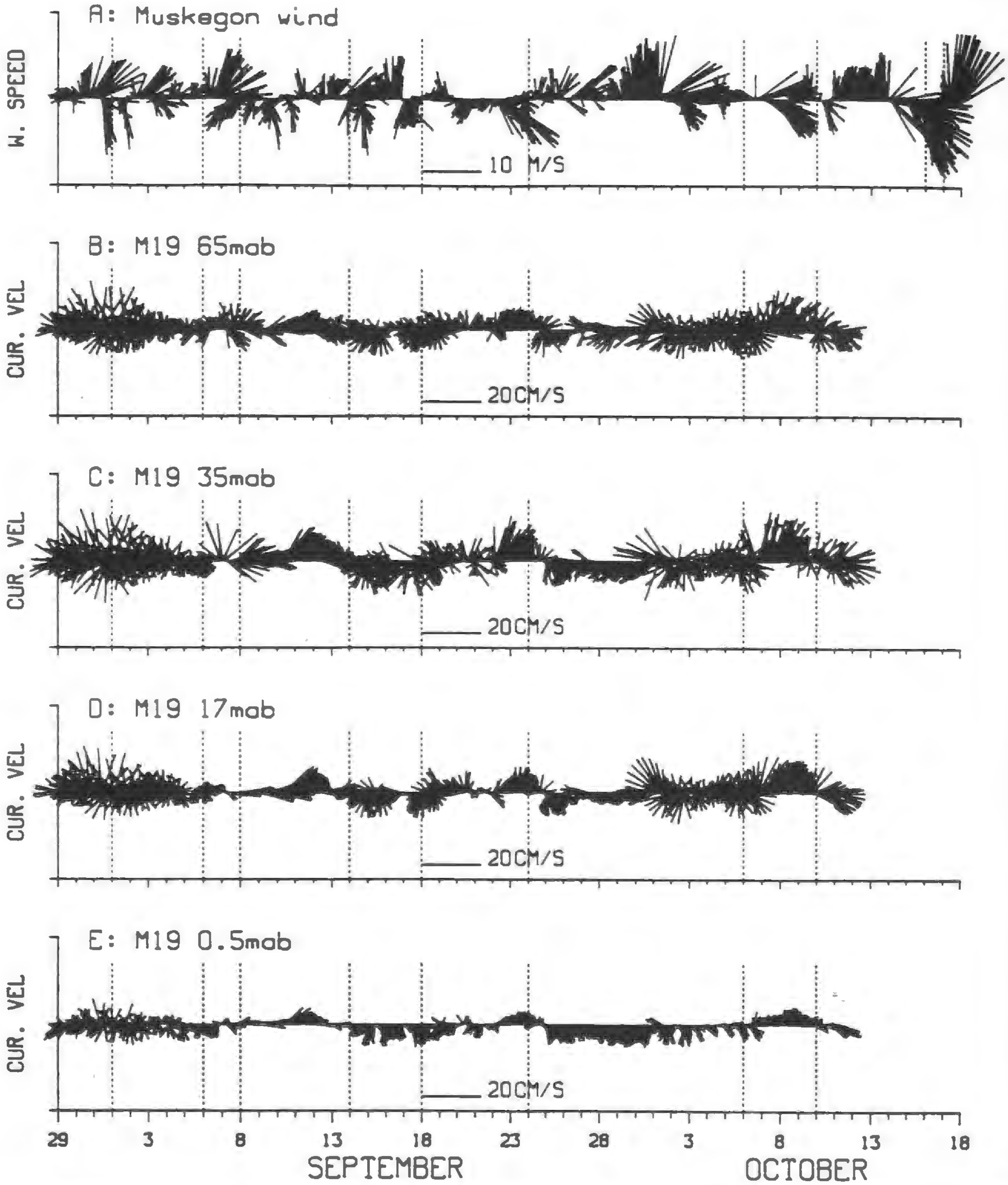

FIG. 7.—Wind observations and current velocities at M19. The current velocities have been rotated 40° clockwise so that alongshore is up and down and offshore is to the left. The convention is that the wind and currents go in the direction of the line, so the wind on 29–30 September blew from the south to the north. The dotted vertical lines separate the upwelling and downwelling events listed in Table 3. A) Wind at the weather station at the entrance of Muskegon Harbor. B) Current velocity 65 mab. C) Current velocity 35 mab. D) Current velocity 17 mab. E) Current velocity 0.5 mab.

tom, and the relatively small waves (maximum period is about 6 s) means that only very severe storms will produce bottom resuspension at depths greater than about 30 m. During the unstratified period resuspension events appear to occur more frequently and at greater depths (Hawley et al. 1996) because of higher wind speeds and breakdown of the thermocline. Our observations are similar in some ways to those made on the continental shelf, where numerous investigations have shown that wave-induced sediment resuspension occurs frequently (Churchill et al. 1988; Lyne et al. 1990; Churchill et al. 1996; Lynch et al. 1997) during the winter, but much less frequently during the spring and summer. The correspondence between our observations and those made on the continental shelf is not exact, however. Churchill et al. (1988) also noted the occurrence of high SPM episodes at the shelf edge during the offshore movement of thermal fronts. The movement of these fronts is analogous in many ways to our downwelling events, but we did not observe any offshore transport of material except in shallow water. However, conditions may be quite different on the west side of the lake, where the greatest wave activity is associated with downwelling events.

CONCLUSIONS

Our observations support none of the three hypotheses stated in the introduction. Although wave-induced bottom resuspension occurs fairly frequently in shallow (13 m) water, it occurs only rarely at the edge of the lake shelf (28 m) during the stratified period, and there is no indication of current-induced resuspension at the offshore stations. Thus there is no evidence that the BNL is maintained by local resuspension due to either bottom currents or surface waves during the stratified period. Some offshore transport of material resuspended in the nearshore area does occur during downwelling events, but we did not observe direct transport of material across the thermocline into the hypolimnion even during strong downwellings. Thus it is unlikely that offshore transport of material by downwelling currents is a direct source of material to the BNL—at least at this site. On the western side of the lake, where wave action is likely to be more intense during downwellings, offshore transport of suspended material may occur. During upwellings suspended material in the BNL is transported onshore into the epilimnion. Although the currents are not strong enough to produce local resuspension, the high levels of BAC associated with the passage of the cold front indicate that some material in addition to that in the offshore BNL is being transported onshore. Although we cannot identify the source of this material from our observations, internal wave action may be important. Changes in the BAC at the offshore stations are due mostly to changes in the structure of the BNL on a regional scale rather than to local conditions. On short time scales these changes may also be due in large part to the effects of internal waves.

ACKNOWLEDGMENTS

We thank the crew of the R/V *Shenehon* and Andy Winkelman for assistance during deployment and retrieval of our moorings, and the technical staff of the Great Lakes Environmental Research Laboratory for calibrating the instruments. Weather data were provided by Clyde Sweet. Thanks also go to Bob Venteklassen of the City of Muskegon Water Filtration Plant for the water intake data. The manuscript was considerably improved by the thoughtful reviews of Dave Drake, Barry Lesht, and Pat Wiberg. This work was supported by the Environmental Protection Agency's Lake Michigan Mass Balance Study under interagency agreement DW131671701. This is GLERL contribution # 1045.

REFERENCES

Baker, J.E., and Eisenreich, S.J., 1989, PCBs and PAHs as tracers of particulate dynamics in large lakes: Journal of Great Lakes Research, v. 15, p. 84–103.

Bell, G.L., and Eadie, B.J., 1983, Variations in the distribution of suspended particles during an upwelling event in Lake Michigan in 1980: Journal of Great Lakes Research, v. 9, p. 559–567.

Blanton, J.O., 1975, Nearshore lake currents measured during upwelling and downwelling of the thermocline in Lake Ontario: Journal of Physical Oceanography, v. 5, p. 111–124.

Bogucki, D., Dickey, T., and Redekopp, L.G., 1997, Sediment resuspension and mixing by resonantly generated internal solitary waves: Journal of Physical Oceanography, v. 27, p. 1181–1196.

Boyce, F.M., Donelan, M.A., Hamblin, P.F., Murthy, C.R., and Simons, T.J., 1989, Thermal structure and circulation in the Great Lakes: Atmosphere-Ocean, v. 27, p. 607–642.

Chambers, R.L., and Eadie, B.J., 1981, Nepheloid and suspended particulate matter in southeastern Lake Michigan: Sedimentology, v. 28, p. 439–447.

Churchill, J.H., Biscaye, P.E., and Aikman III, F., 1988, The character and motion of suspended particulate matter over the shelf edge and upper slope off Cape Cod: Continental Shelf Research, v. 8, p. 789–809.

Churchill, J.H., Wirick, C.D., Flagg, C.N., and Pietrafesa L.J., 1996, Sediment resuspension over the continental shelf east of the Delmarva Peninsula: Deep-Sea Research, v. 41, p. 341–363.

Colman, S.M., and Foster, D.S., 1994, A sediment budget for southern Lake Michigan: source and sink models for different time intervals: Journal of Great Lakes Research, v. 20, p. 215–228.

Csanady, G.T., and Scott, J.T., 1974, Baroclinic coastal jets in Lake Ontario during IFYGL: Journal of Physical Oceanography, v. 4, p. 524–541.

Eadie, B.J., Chambers, R.L., Gardner, W.S., and Bell, G.L., 1984, Sediment trap studies in Lake Michigan: resuspension and chemical fluxes in the southern basin: Journal of Great Lakes Research, v. 10, p. 307–321.

Edgington, D.V., and Robbins, R.A., 1990, Time scales of sediment focusing in large lakes as revealed by measurement of fallout Cs-137, *in* Tilzer, M.M., ed., Large Lakes: Ecological Structure and Function: New York, Springer-Verlag, p. 210–233.

Grant, W.D., and Madsen, O.S., 1979, Combined wave and current interaction with a rough bottom: Journal of Geophysical Research, v. 87, p. 1797–1808.

Halfman, B.M., and Johnson, T.C., 1989, Surface and benthic nepheloid layers in the western arm of Lake Superior, 1983: Journal of Great Lakes Research, v. 15, p. 15–25.

Hawley, N., and Lesht, B.M., 1995, Does local resuspension maintain the benthic boundary layer in Lake Michigan?: Journal of Sedimentary Research, v. A65, p. 69–76.

Hawley, N., and Murthy, C.R., 1995, The response of the benthic nepheloid layer to a downwelling event: Journal of Great Lakes Research, v. 21, p. 641–651.

Hawley, N., and Zyren, J.E., 1990, Transparency calibration for Lake St. Clair and Lake Michigan: Journal of Great Lakes Research, v. 16, p. 113–120.

Hawley, N., Wang, X., Brownawell, B., and Flood, R., 1996, Resuspension of bottom sediments in Lake Ontario during the unstratified period, 1992–1993: Journal of Great Lakes Research, v. 22, p. 707–721.

Kim, S.-C., Wright, L.D., and Kim, B.-O., 1997, The combined effects of synoptic-scale and local-scale meteorological events on bed stress and sediment transport on the inner shelf of the Middle Atlantic Bight: Continental Shelf Research, v. 17, p. 407–433.

Lesht, B.M., 1989, Climatology of sediment transport on Indiana Shoals, Lake Michigan: Journal of Great Lakes Research, v. 15, p. 486–497.

Lesht, B.M., and Hawley, N., 1987, Near-bottom currents and suspended sediment concentration in southeastern Lake Michigan: Journal of Great Lakes Research, v. 13, p. 375–386.

Lynch, J.F., Gross, T.F., Sherwood, C.R., Irish, J.D., and Brumley, B.H., 1997, Acoustical and optical backscatter measurements of sediment transport in the 1988–1989 STRESS experiment: Continental Shelf Research, v. 17, p. 337–366.

Lyne, V.D., Butman, B., and Grant, W.D., 1990, Sediment movement along the U.S. east coast continental shelf—II. Modeling suspended sediment concentration and transport rate during storms: Continental Shelf Research, v. 10, p. 429–460.

Miller, M.C., McCave, I.N., and Komar, P.D., 1977, Threshold of sediment motion under unidirectional currents: Sedimentology, v. 24, p. 507–527.

Mitchener, H., Torfs, H., and Whitehouse, R., 1996, Erosion of mud/sand mixtures: Coastal Engineering, v. 29, p. 1–25.

Mortimer, C.H., 1980, Inertial Motion and Related Internal Waves in Lake Michigan and Lake Ontario as Responses to Impulsive Wind Stresses: Milwaukee, Wisconsin, Center for Great Lakes Studies, Special Report 37, 192 p.

Mudroch, A., and Mudroch, P., 1992, Geochemical composition of the nepheloid layer in Lake Ontario: Journal of Great Lakes Research, v. 18, p. 132–153.

Panagiotopoulos, I., Voulgaris, G., and Collins, M.B., 1997, The influence of clay on the threshold of movement of fine sandy beds: Coastal Engineering, v. 32, p. 19–43.

Rea, D. K., Owen, R.M., and Meyers, P.A., 1981, Sedimentary processes in the Great Lakes: Reviews of Geophysics and Space Physics, v. 19, p. 635–648.

Rosa, F., 1985, Sedimentation and sediment resuspension in Lake Ontario: Journal of Great Lakes Research, v. 11, p. 13–25.

Sandilands, R.G., and Mudroch, A., 1983, Nepheloid layer in Lake Ontario: Journal of Great Lakes Research, v. 9, p. 190–200.

Schwab, D.J., and Beletsky, D., 1997, Hydrodynamic modeling program in the Lake Michigan Mass Balance Project: Workshop on Research Needs for Coastal Pollution in Urban Areas, University of Wisconsin–Milwaukee/ National Science Foundation, Milwaukee, Wisconsin p. 14–22.

Sly, P.G., 1994, Sedimentary processes in lakes, *in* Pye, K., ed., Sediment Transport and Depositional Processes: Oxford, England, Blackwell, p. 157–191.

Transport Canada, 1991, Wind and Wave Climate Atlas III: Ottawa, Ontario, The Great Lakes Transportation Development Centre, Policy and Coordination Group, Transport Canada, 402 p.

Received 31 July 1997; accepted 24 April 1998.